Journal of Medical Research and Innovation

An Open Peer Reviewed Journal...

JMRI

Accepted and to be published in Journal of Medical Research and Innovation

Contrast media volume is significantly related to patient lung volume during CT pulmonary angiography when employing a patient-specific contrast protocol

1. Charbel Saade, PhD

Faculty of Health Sciences, American University of Beirut Medical Center, Beirut, Lebanon. P.O.Box: 11-0236 Riad El-Solh, Beirut, 1107 2020, Lebanon.

Email: mdct.com.au@gmail.com

2. Youssef Ghosn

Diagnostic Radiology Department, American University of Beirut Medical Center, Beirut, Lebanon. P.O.Box: 11-0236 Riad El-Solh, Beirut, 1107 2020, Lebanon.

Email: yg05@aub.edu.lb

3. Ghina Alfout

Diagnostic Radiology Department, American University of Beirut Medical Center, Beirut, Lebanon. P.O.Box: 11-0236 Riad El-Solh, Beirut, 1107 2020, Lebanon.

Email: ghina-alfout@hotmail.com

4. Mustafa Zuhair Mahmoud, PhD

College of Applied Medical Sciences, Salman bin Abdulaziz University, Radiology and Medical Imaging Department

P.O. Box: 422, Postal Code: 11942

E-mail address: m.alhassen@psau.edu.sa; zuhairmustafa4@hotmail.com

Al-Kharj - Saudi Arabia

5. Mohammad Ahmmad Rawashdeh, Ph.D
Department of Allied Medical Sciences, Jordan University of Science and Technology.
Phone: (+962)2-7201000 Ext: 26931 Address: P.O.Box: 3030, Department of Allied Medical Sciences. Jordan University of Science and Technology Irbid 22110, Jordan
Email: marawashdeh@just.edu.jo

6. Lina Karout, MD
Faculty of Health Sciences, American University of Beirut Medical Center, Beirut, Lebanon. P.O.Box: 11-0236 Riad El-Solh, Beirut, 1107 2020, Lebanon.
Email: lk74@aub.edu.lb

7. Diamond Ghieh, MD
Diagnostic Radiology Department, American University of Beirut Medical Center, Beirut, Lebanon. P.O.Box: 11-0236 Riad El-Solh, Beirut, 1107 2020, Lebanon.
Email:

8. Fadi El-Merhi, MD
Department of Imaging, Dana-Farber Cancer Institute and Harvard Medical School, Boston, MA, USA, Department of Radiology, Brigham and Women's Hospital and Harvard Medical School, Boston, MA, USA
E-mail: FEL-MERHI@BWH.HARVARD.EDU

Corresponding author: Fadi El-Merhi, MD
Department of Imaging, Dana-Farber Cancer Institute and Harvard Medical School, Boston, MA, USA
Department of Radiology, Brigham and Women's Hospital and Harvard Medical School, Boston, MA, USA
E-mail: FEL-MERHI@BWH.HARVARD.EDU

Disclaimers: *None*

Source(s) of support: *None*

Word count: *5685*
Number of figures and tables: *4 figures and 5 tables*

Conflict of interest

Charbel Saade declares that he has no conflict of interest. Youssef Ghosn declares that he has no conflict of interest. Ghina Alfout declares that she has no conflict of interest. Mustafa Zuhair Mahmoud declares that he has no conflict of interest. Mohammad Ahmmad Rawashdeh declares that he has no conflict of interest. Lina Karout declares that she has no conflict of interest. Diamond Ghieh declares that she has no conflict of interest. Fadi El-Merhi declares that he has no conflict of interest.

Compliance with Ethical Standards:

· No funding was needed for this article

· Ethical approval: This article does not contain any studies with human participants or animals performed by any of the authors.

· Informed consent: Informed consent was obtained from all individual participants included in the study.

Article details

DOI : 10.32892/jmri.207

Volume & Issue : Vol 4 No 2 (2020)

Page No.: e000207

How to Cite

Saade C, Ghosn Y, Alfout G, Mahmoud M, Rawashdeh M, Karout L, Ghieh D, El-Merhi F. Contrast media volume is significantly related to patient lung volume during CT pulmonary angiography when employing a patient-specific contrast protocol. J Med Res Innov. 2020;4(2):e000207. DOI: 10.32892/jmri.207

Contrast media volume is significantly related to patient lung volume during CT pulmonary angiography when employing a patient-specific contrast protocol

Abstract

Purpose: The purpose of this study is to investigate the relationship between contrast media volume and patient lung volume when employing a patient-specific contrast media formula during pulmonary computed tomography angiography (CTA).

Materials and methods: IRB approved this retrospective study. CTA of the pulmonary arteries was performed on 200 patients with suspected pulmonary embolism (PE). The contrast media volume (CMV) was calculted by employing a patient-specific contrast formula. Lung volume was quantified employing semi-automated lung software that calculated lung volumes (intellispace -Philips). The mean cross-sectional opacification profile of central and peripheral pulmonary arteries and veins were measured for each patient and arteriovenous contrast ratio (AVCR) calculated for each lung segment. Mean body mass index (BMI) and lung volume were quantified. Receiver operating (ROC) and visual grading characteristics (VGC) measured reader confidence in emboli detection and image quality respectively. Inter and intra-observer variations were investigated employing Cohen's kappa methodology.

Results: Results showed that the mean pulmonary arterial opacification of the main pulmonary circulation (343.88±73HU), right lung; upper (316.51±23HU), middle (312.5±39HU) and lower (315.23±65HU) lobes and left; upper (318.76±83HU), and lower (321.91±12HU) lobes. The mean venous opacification of all pulmonary veins was below 182±72HU. AVCR was observed at all anatomic locations ($p<0.0002$) where this ratio was calculated. Moreover, larger volumes of contrast significantly correlated with larger lung volumes ($r=0.89$, $p<0.03$) and radiation dose ($p<0.03$). VGC and ROC analysis demonstrated increased area under the curve: 0.831 and 0.99 respectively ($p<0.02$). Inter-observer variation was observed as excellent ($\kappa = 0.71$). We conclude that increased CMV is significantly correlated to increased patient lung volume and radiation dose when employing a patient-specific contrast formula. The effects patient habitus is highlighted.

Key Words: contrast media, contrast protocol, computed tomography, lung volume, pulmonary angiography

Introduction

Although the gold standard in pulmonary embolism diagnosis is still angiopulmonography, computed tomography pulmonary angiography (CTPA) protocols have witnessed a surge in thrombus detection at a specificity and sensitivity approaching 100% with additional benefits of non-invasiveness and accessibility (1). Since this efficacy is largely dependent on effective contrast media volume (CMV) administration, studies have been extensively conducted on contrast administration protocols (2-8). These studies have found that visualization of the pulmonary vasculature is significantly improved when using a simple patient-specific formula (1, 7, 9), which also allows CMV to be reduced along with the potential risk of contrast induced nephropathy (1).

Studies performed on adult patients with normal pulmonary functioning demonstrated an air/tissue relationship approaching a 7:3 ratio of air to lung parenchyma (10); other studies noticed that an increase in total lung volume is concomitant with an increase in the volume of pulmonary blood and pulmonary extravascular water (11). To our knowledge, there have been no studies to date that compares CMV with patient lung volume employing a reduced patient-specific formula. The aim of the study is to investigate the relationship between CMV and patient lung volume when employing a patient-specific contrast media formula during CTPA. Our results could be used as a foundation for further research on lung volume specific CTPA protocols.

Materials and Methods

Study Population

The institutional review board approved this study and written informed consent was waived since all studies were clinically indicated and patient data was evaluated retrospectively. Two hundred consecutive patients with high clinical suspicion of acute pulmonary embolism (PE) were examined over a 6-month period between August 2018 and January 2019. The indication for CTPA was suspected PE based on clinical information (chest pain, dyspnea, hypoxia, calf pain or known deep vein thrombosis (DVT), risk factors for PE) and/or laboratory information (positive d-dimer > 0.8 mg/L). All patients with a positive PE in this study received anticoagulation therapy and due to the nature of the suspected condition, all patients were scanned. Inclusion criteria were patient with suspected PE as per the criteria mentioned above, who underwent CTPA. Patient with no suspected PE, or patient with PE who did not undergo CTPA were excluded. There were no patients in the study that had renal insufficiency and/or contra-indications to iodinated contrast media. The diagnosis and treatment were in adherence with amercan collage of cardiology (ACC) guidelines for the diagnosis and managent of pulmonary embolism.

Ethical approval:

All procedures performed in studies involving human participants were in accordance with the ethical standards of the American university of Beirut's institutional review board (IRB) and with the 1964 Helsinki declaration and its later amendments or comparable ethical standards. Informed consent was waived since all studies were clinically

indicated, patient data contained no identifiable information and was evaluated retrospectively.

Image Acquisition

CTPA was performed using a 256-channel computed tomography scanner (Philips Brilliance iCT, Philips Healthcare, The Netherlands). Patients were positioned supine with arms resting on the gantry above the head. Anterior-posterior scout were performed, with a scan range from the apices (2 cm above the 1st rib) to the diaphragm (2 cm below the lowest costophrenic recess). Breath-hold, with a mouth open breathing technique were employed in order to reduce hyperventilation and Valsalva. Scan range was from the lung apices to the costophrenic angles. CT scan parameters employed in each protocol were: detector width of 256×0.625 mm, pitch of 0.981:1 ratio, rotation time of 0.27 sec, 100 kVp, 140 mA, with x,y and z-axis modulation (DoseRight), craniocaudal scan direction and model based iterative reconstruction (IMR2).

Contrast Media Administration

Contrast Bolus Geometry

Vessel opacification for all cases was measured by placing a region of interest (ROI) over the main pulmonary trunk. A time attenuation curve in Hounsfield units (HU) was calculated and the desired peak opacification was recorded. The patient-specific protocol employed the test bolus technique (12) where the ROI was plotted inside the main pulmonary trunk with a small amount of contrast material (5 mL) injected at the same rate

as the main bolus. This ROI assessed the time to peak (TTP) and determined the arteriovenous circulation time for pulmonary vasculature (12-14).

Contrast Media Acquisition

Contrast and saline chaser were injected with an automated dual barrel power injector (CT Emotion, Ullrich, Germany) via a 20G venous catheter in the right arm (15, 16). The patient-specific contrast formula employed iodinated contrast (Omnipaque 350 mgI/mL; General Electric, USA) intravenously injected at a flow rate of 4.5 mL/s. Contrast media volume was calculated according to an empirically derived formula (17): CV=(ST+TTP-OVWP)×FR. Where ST is the scan time (s), TTP (s) is as described above, OVWP is the optimal venous washout phase (6s), and FR is the flow rate (mL/s). ST differs for each patient based on the distance between the apices and diaphragm of the thorax. Patients were excluded if they were unable to have a right sided injection site in the cubital fossa with a flow rate of 4.5 mL/s.

Radiation Dose Measurement

For each of the CT scans, individual effective dose (E_{ff} [mSv]) was calculated from the dose-length products (DLP [mGy × cm]), which were recorded from the patient protocol. A normalized conversion factor (k [mSv / mGy × cm]) for the chest—0.014 mSv/mGy × cm—was used to calculate the E_{ff} (18): E_{ff} = DLP x k (4).

Image assessment

Technical inclusion criteria ensuring correct scan range and anatomical inclusion of the origin, pathway and termination of the pulmonary vasculature were applied to all cases by two expert radiologists (not included in the study proper). Quantitative measurements of all images were performed using a primary reporting workstation (Intellispace,Philips Healthcare, Netherlands) with a GSDF-calibrated 3 megapixel monitor. Illumination was adjusted at 25 to 32 lux (19), with a calibrated photometer (chroma meter CL-200).

Quantitative Analysis

Opacification in HU was measured for all cases in the trans-axial images within the largest circular ROI that would fit within the lumen and exclude the vessel wall. The mean cross-sectional opacification profile of 8 central segments and 11 peripheral pulmonary arteries were measured. In cases where PE was identified, care was taken not to include the emboli within the measurements. Arterial and venous measurements took place at the heart, pulmonary trunk, segmental and sub segmental pulmonary vasculature and each measurement was no less than 2 mm in diameter (Figure 1). The location of the arteries and veins were as follows:central pulmonary vasculature (trunk, right and left pulmonary arteries and left superior and inferior pulmonary veins); pulmonary segments; right upper lobe (anterior and posterior), right middle lobe (lateral and medial), right lower lobe (anterior and posterior basal), left upper lobe (apico-posterior and inferior lingular) and left lower lobe (anteromedial basal and posterior basal); superior vena cava (SVC).

Adjacent to the arterial pathways, the venous measurements were performed in the same axial plane. Image contrast between arteries and veins was expressed as a ratio of HU values (artery/vein) at each anatomical level and denoted as the arteriovenous contrast ratio AVCR (20).

Lung volume parenchyma and airway volumes were measured by quantitative volumetric analysis (Figure 2) on the CTPA imaging sequence using the Philips Intellispace lung segmentation software (v6.0.3.12200, Best, The Netherlands).

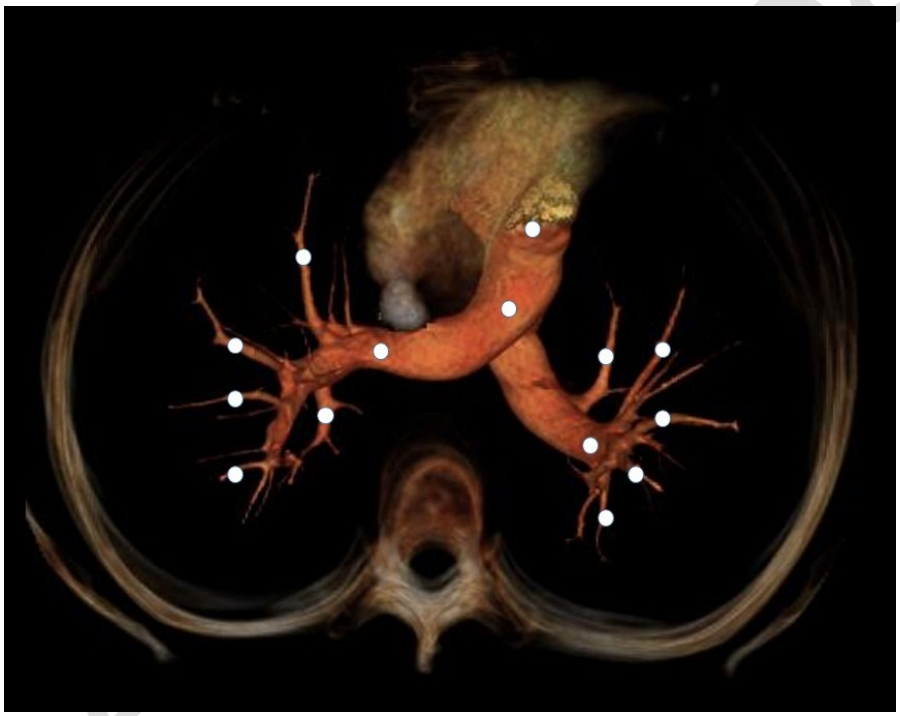

Figure 1: anatomical location of measurements of the pulmonary vasculature

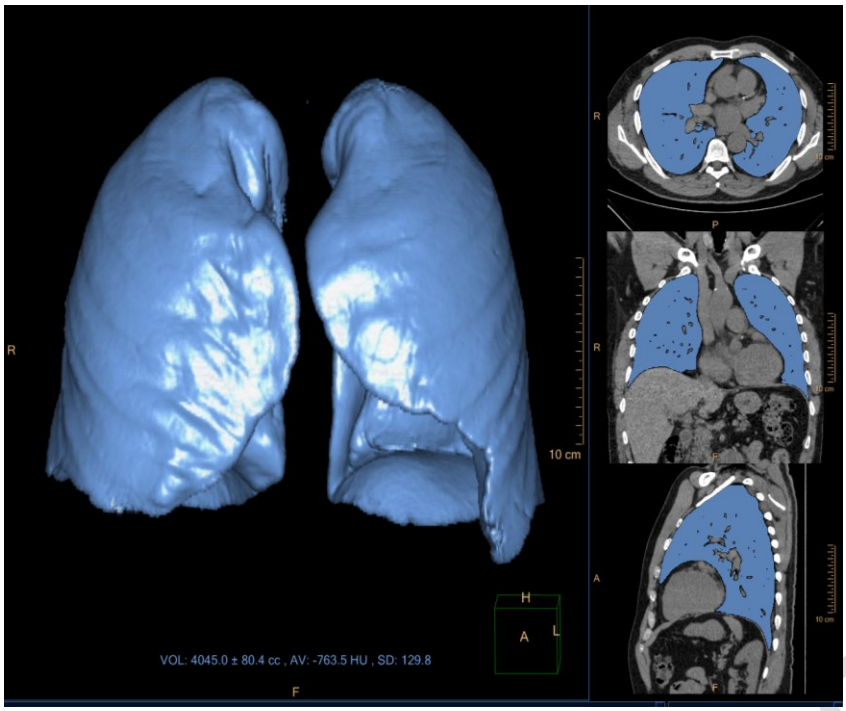

Figure 2: Lung volume analysis

Diagnostic Efficacy

The multi-reader analysis consisted of two cardiothoracic radiologists who had been certified by the American Board of Radiology and The Royal College of Radiologists for a mean number of 8.9 years (minimum, 3 years; maximum, 18 years). All reviewers were specialists in cardiothoracic imaging and each observer was allowed to manipulate the window level of the images.

ROC Analysis

Receiver operating characteristic (ROC) methodology was employed to illustrate radiologist confidence intervals to detect pathology. A score of 1 to 2 was assigned to each image, where 1 indicates positive for pathology detection and 2 indicates negative for pathology detection of PE. All cases were randomly allotted with the number of normal

(n=87) and abnormal (n=113) cases. The abnormal cases demonstrated an array of vascular disease that were defined by two radiologists' reports (based on complete patient series, previous and subsequent examinations and clinical indications). All pathology was visible on the transaxial images and the prevalence of pathology was not revealed to the observers. Technical criteria ensuring correct scan range and anatomical inclusion were considered (not included in the study proper) to ensure that all images displayed an acceptable level of quality before they were included in the analysis.

VGC analysis

The VGC method of Bath and Mansson (21) was used to illustrate viewer assessment of image quality based on the visibility of normal anatomy. Specifically, for this work, the presence of contrast media filling was recorded for pulmonary arterial system using a five-point classification scale where score 1 indicated no contrast media filling within the pulmonary vasculature and 5 represented complete filling.

Inter- and intra-reader variability

The inter- and intra-observer agreements were calculated using Cohen κ analysis. A k value 0.60 to 1, 0.41 to 0.60, 0.21 to 0.40, and less than 0.20 was considered excellent, moderate, fair, and poor agreement, respectively.

Statistical Analysis

Continuous variables were described with mean ± standard deviation (SD). The analysis of variance (ANOVA) was used to compare the means across the tertiles of contrast volume. The association between contrast volume and measured variables was evaluated through simple linear regression. Analyses were conducted using SPSS 22 for Windows (SPSS Inc, Chicago, IL). Results were considered statistically significant if $p \leq 0.05$ with a 95% confidence interval and a power of 0.8. ROC and VGC were employed to measure the confidence intervals in pathology detection and image quality respectively. Jackknife Free-response (JAFROC) assessment of diagnostic systems continues to gain acceptance in areas related to the detection, localization and classification of one or more "abnormalities" within a subject.

Results

Patient Demographics

There was no significant change in CMV with gender and age, however, CMV increased with increasing body weight ($p<0.004$) and BMI ($p<0.01$) (Table 1). Additionally, the effective radiation dose also increased from low contrast media volumes (0-10mL) to higher contrast media volumes (60-70 mL) ($p<0.03$) incrementally.

Table 1: patient demographics

Patient Parameters	Contrast Volume Range (mL)							
	0-10	10-20	20-30	30-40	40-50	50-60	60-70	P value
Male	0	3	9	63	15	8	1	> 0.096
Female	2	3	5	39	29	20	3	> 0.338
Total	2	6	14	102	44	28	4	> 0.077
Age (years)*	51.23±11.23	64 ± 19.83	67 ± 18.34	42 ± 12.24	48 ± 19.67	55 ± 42.28	59 ± 23.22	> 0.068
Height (cm)*	172.16 ± 2.13	167 ± 18.51	181 ± 24.33	177± 48.73	182 ± 13.11	173 ± 26.41	175 ± 9.77	> 0.078

Weight (kg)*	51 ± 9.12	52 ± 13.81	58 ± 33.18	73 ± 16.81	75 ± 12.93	81 ± 22.67	82 ± 13.46	< 0.004
BMI (kg/m2)	25.32 ± 8.22	24 ± 6.67	25 ± 3.89	26 ± 4.38	25 ± 9.22	27 ± 4.54	27 ± 9.91	< 0.01
Scan Time (sec)	3.22 ± 1.2	3.77 ± 1.9	3.99 ± 1.4	4.11 ± 1.1	4.21 ± 1.7	4.38 ± 0.9	4.39 ± 0.7	> 0.066
Scan Range (cm)	52.12 ± 1.07	52.54 ± 1.78	53.17 ± 1.81	53.48 ± 3.22	53.71 ± 4.91	53.91 ± 4.03	54.16 ± 3.12	> 0.067
E_{ff} Dose (mSv)	2.41 ± 0.62	2.46 ± 1.47	2.59 ± 0.75	2.79 ± 1.13	3.19 ± 0.44	3.59 ± 0.49	3.91 ± 0.22	< 0.003

Note – Data are mean ± standard deviation, $p<0.05$, statistically significant with ANOVA

Image acquisition and contrast media volume

There was no statistical significance in mean scan time in each contrast range; 0-10 mL: (3.22 ± 1.2 sec) compared to 60-70 mL: (4.39 ± 1.3 sec), ($p>0.05$)(Table 1). All patients tolerated their assigned contrast material delivery protocol without any related complication.

Quantitative Analysis

The mean pulmonary arterial opacification of the main pulmonary circulation was (343.88±73HU). For the right lung, the mean arterial opacification was: upper lobe (316.51±23HU), middle lobe (312.5±39HU) and lower lobe (315.23±65HU). For the left lung, the mean arterial opacification was: upper lobe (318.76±83HU) and lower lobe (321.91±12HU) (Table 2). The mean venous opacification of all pulmonary veins was below the threshold of 182±72HU (Table 2). Additionally, opacification of the superior vena cava veins was approximatly double that of the mean pulomnary artery opacification. The AVCR ranged from 2.21:1 to 3.83:1 ($p<0.0010$) which demonstrated significant difference between

arterial and venous opacification (Table 3).

Table 2: Mean opacification (HU) of arteries and veins at each anatomical segment during CTPA.

	Anatomical Location	Mean Opacification with SD
Pulmonary Trunk	Mediastinum	362 ± 97
Right main pulmonary artery		337 ± 88
Left main pulmonary artery		323 ± 88
Atrial Vein	Mediastinum	
Right superior		177 ± 73
Right inferior		154 ± 67
Left superior		182 ± 72
Left inferior		157 ± 61
Superior vena cava		606 ± 257
Pulmonary Arteries		
Right superior anterior	Right upper	320 ± 87
Right superior posterior	lobe	313 ± 83
Right medial		311 ± 93
Right lateral	Right middle	314 ± 86
Right anterior-basal	lobe	306 ± 89
Right posterior-basal		325 ± 95
	Right lower	
Left apico-posterior	lobe	314 ± 79
Left inferior lingular		323 ± 86
Left anteromedial basal		319 ± 82
Left posterior-basal	Left upper lobe	323 ± 83
Pulmonary Veins		
Right superior anterior	Left lower lobe	112 ± 79
Right superior posterior		122 ± 78
Right medial		95 ± 62
Right lateral		101 ± 60
Right anterior-basal	Right upper	92 ± 61
Right posterior-basal	lobe	96 ± 59
Left apico-posterior	Right middle	141 ± 80
Left inferior lingular	lobe	146 ± 77
Left anteromedial basal		120 ± 61
Left posterior-basal	Right lower lobe	111 ± 62

	Left upper lobe	
	Left lower lobe	

Note—Data are mean ± standard deviation (SD), $p<0.05$, statistically significant with ANOVA

Table 3: Mean opacification (HU) profile of artery and vein at each anatomical level and the ratio of the AVCR.

Anatomical Level	Anatomical Location	Artery	Vein	Ratio	P value
Right superior anterior	Right Upper Lobe	320 ± 87	112 ± 79	2.86	<0.0001
Right superior posterior		313 ± 83	122 ± 78	2.65	<0.0001
Right medial	Right Middle Lobe	311 ± 93	95 ± 62	3.27	<0.0001
Right lateral		314 ± 86	101 ± 60	3.10	<0.0001
Right anterior-basal	Right Lower Lobe	306 ± 89	92 ± 61	3.33	0.0002
Right posterior-basal		325 ± 95	96 ± 59	3.38	0.0002
Left apico-posterior	Left Upper Lobe	314 ± 79	141 ± 80	2.23	<0.0001
Left inferior lingular		323 ± 86	146 ± 77	2.21	<0.0001
Left anteromedial basal	Left Lower Lobe	319 ± 82	120 ± 61	2.66	<0.0001
Left posterior-basal		323 ± 83	111 ± 62	2.91	<0.0001

Note—Data are mean ± standard deviation, p<0.05, statistically significant with ANOVA

Lung Volume vs. Contrast volume in patient specific contrast formula

When employing the patient-specific formula, increase in CMV positively correlated with increased total lung volume (*r =0.89,* p< 0001). As expected, total lung

volume increased with increasing mean anteroposterior and lateral lung diameters. Therefore, increased lung volume, anteroposterior, and lateral chest diameters are correlated with increased CMV (Table 4).

Table 4: Mean lung volumes (mL), contrast media (mL) and chest diameters (mm).

CMV Range (mL)	RLV (mL)	Left LV (mL)	Total LV (mL)	Total LV per CM (mL)	Mean AP Diameter (mm)	Mean LAT Diameter (mm)
0 – 10 (2)	1482.71 ± 32.52	1367.97 ± 53.42	2849.97 ± 46.12	569.34 ± 31.19	265.37 ± 09.12	185.18 ± 13.02
10 – 20 (6)	1593.86 ± 47.11	1358.22 ± 81.34	2951.22 ± 62.28	196.18 ± 28.03	277.16 ± 19.87	193.27 ± 68.41
20 – 30 (14)	1618.13 ± 19.83	1575.92 ± 63.19	3193.92 ± 48.19	127.63 ± 16.18	283.44 ± 16.11	198.22 ± 17.61
30 – 40 (102)	1690.44 ± 33.69	1745.14 ± 28.12	3435.14 ± 29.73	98.17 ± 11.28	302.21 ± 19.19	208.38 ± 19.76
40 – 50 (44)	1809.5 ± 59.85	2110.22 ± 31.6	3919.46 ± 32.81	87.04 ± 15.32	306.57 ± 28.45	217.26 ± 28.32
50 – 60 (28)	2305.5 ± 55.52	1857.50 ± 45.5	4162.10 ± 52.57	69.38 ± 03.12	322.28 ± 16.32	225.18 ± 29.22
60 – 70 (4)	2403.8 ± 42.16	1798.14 ± 31.9	4201.08 ± 13.22	64.63 ± 02.29	329.10 ± 22.58	231.92 ± 18.47

Note – Data are mean (±) indicate the standard deviation

However, we further stratified CMV groups into tertiles (3 groups) to equally distribute the number of patients across each group unlike in table 4. Regression analysis was performed for each CMV group relative to lung volume. By comparing CMV 1(< 32mL) and 2 (>33 - <50 mL) demonstrated significant changes in the right and left lungs ($p<0.006$) (Table 5). Also, when comparing group 2 (>37 - <40 mL) with group 3 (> 41mL), statistical significance was seen with increasing lung volumes in both right and left lung ($p<0.001$) as well as an increase in effective radiation dose ($p<0.04$) (Table 5). Interestingly, after regression analysis was performed, weight and BMI had no statistical significance association with increased lung volume and CMV.

Table 5: Contrast media volume ranges

Note – (±) indicate the standard deviation, $p<0.05$, statistically significant with ANOVA

		Contrast Media Volume Range (mL)			
	All (n =200)	**<32 (n = 60)**	**33 to 40 (n = 81)**	**>41 (n = 59)**	**P-value**
Right Lung Volume	1843.42 ± 39.67	1564.91 ± 38.31	1749.96 ± 43.82	2354.65 ± 98.23	0.007
Left Lung Volume	1687.59 ± 59.17	1434.38 ± 29.76	1927.68 ± 14.09	1827.82 ± 60.64	0.006
Total Lung Volume	3530.41 ± 98.36	2998.65 ± 47.23	3677.39 ± 102.44	4181.59 ± 130.05	0.001
Weight	78.91 ± 14.78	78.79 ± 16.87	77.76 ± 14.83	80.25 ± 12.48	0.561
Height	1.71 ± 0.09	1.69 ± 0.09	1.72 ± 0.08	1.72 ± 0.09	0.383
Body Mass Index	27.07 ± 4.67	27.53 ± 5.20	26.31 ± 4.16	27.37 ± 4.62	0.383
Anteroposterior Length	298.11 ± 32.64	275.33 ± 32.17	304.05 ± 33.88	286.69 ± 30.90	0.08
Lateral Length	208.48 ± 33.15	192.23 ± 33.15	212.82 ± 34.99	201.55 ± 38.24	0.08
Dose Length Product	163.90 ± 49.22	178.83 ± 61.93	188.38 ± 40.09	164.44 ± 38.71	0.08
Effective Dose	2.31 ± 0.74	1.89 ± 0.93	2.13 ± 0.60	2.60 ± 0.58	0.04

Qualitative Analysis

Visual grading characteristic - the scores were individually graded by the two

readers (R1 and R2) and were expressed as a graph (Figure 3). The sensitivity and specificity were then compared by calculating the area under the curve (AUC) differences from each of the ROC curve analysis. Calculating the difference between each reader, the graphs demonstrated an AUC=0.831, with a 95% confidence interval of 0.71-0.89 ($p<0.02$).

Jacknife free response receiver operating characteristic – the six-point scale demonstrated a significant difference ($p<0.001$) between protocols with mean ROC values demonstrating strong reader confidence between each CMV range (95%CI 0.88-0.99) (figure 4). The number of patient diagnosed with PE was 38 (19%). Kappa analysis - CTPA yielded excellent interobserver agreement ($k = 0.71$) in all ranges. There was a strong positive relationship between mean pulmonary arterial opacification, good image quality and reader confidence in the patient specific protocol ($r = 0.67$, $p < 0.001$).

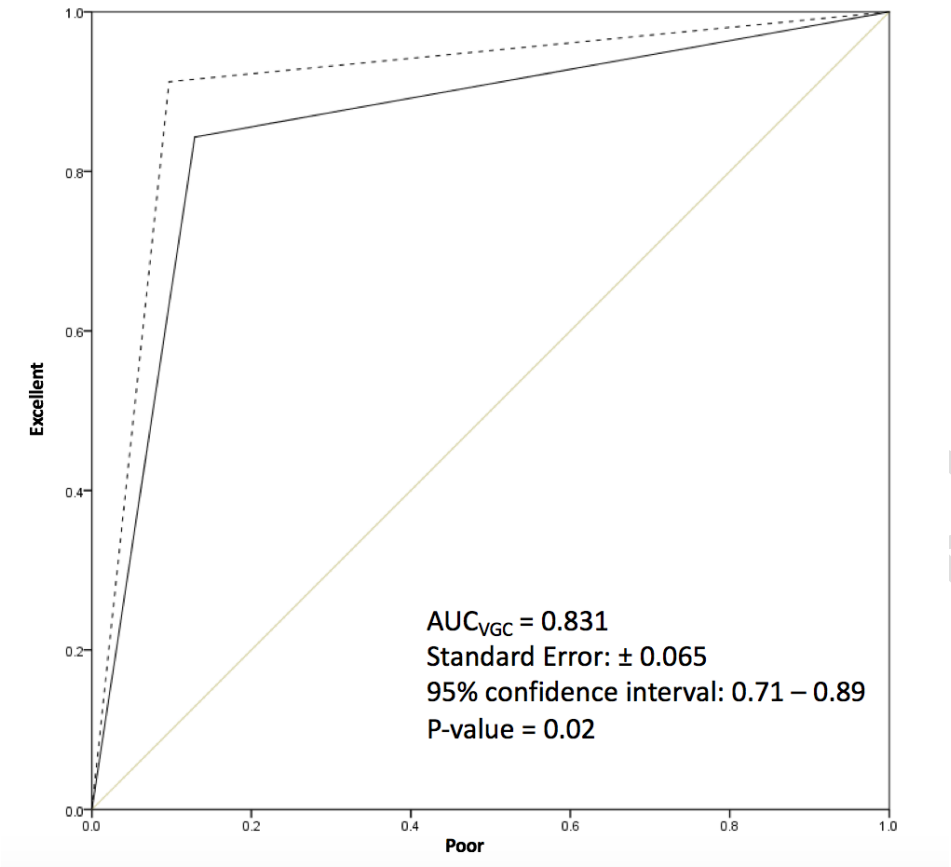

Figure 3: Visual grading characteristic curve. The graph represents positive agreement in image quality during pulmonary CTA. VGC was employed to measure the confidence intervals in image quality assessment by radiologists.

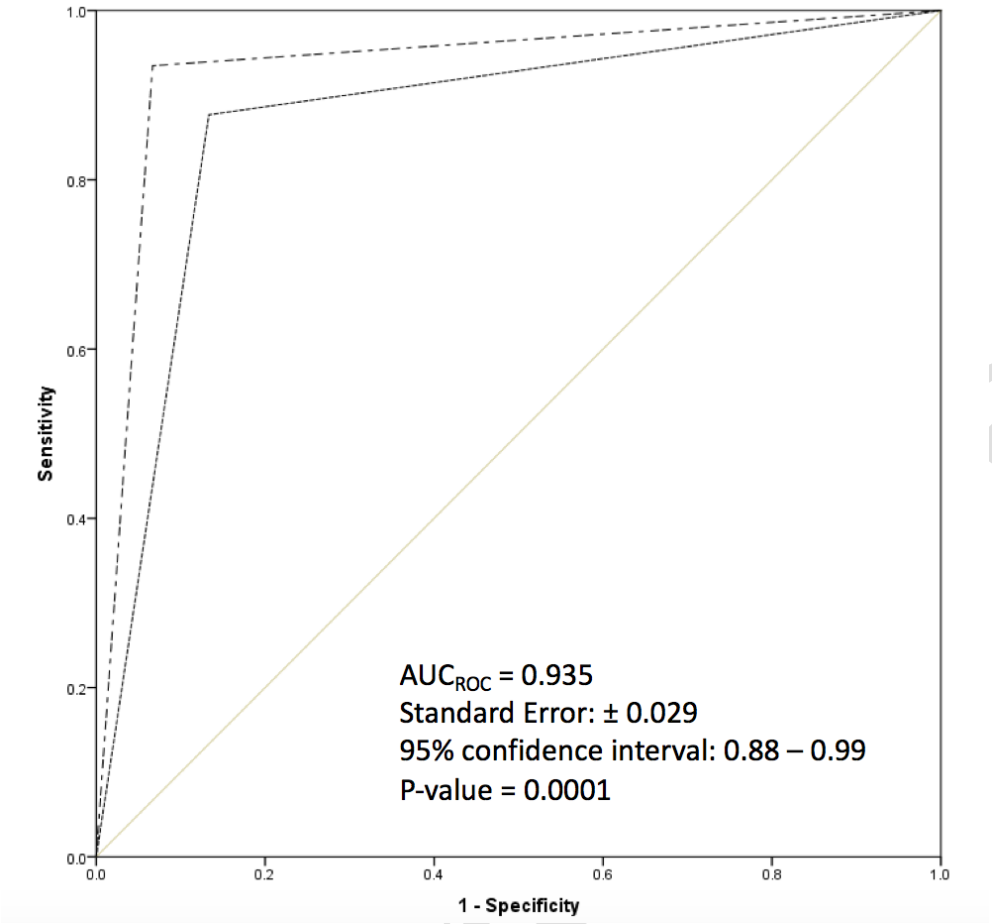

Figure 4: Receiver operating characteristic curve. The graph represents significant sensitivity and specificity in pathology detection at all lung volumes and contrast volumes. ROC was employed to measure the confidence intervals in pathology detection by radiologists.

Discussion

There have been considerable studies carried out to reduce radiation dose via reduction of radiation output, fixed CMV and reduced contrast media concentrations during CTA (22-24). Additionally, weight-based contrast media protocols have been considerably used to perform consistent optimal image quality during CTPA, but at the

cost of larger CMV for considerably larger patients (25). However, until recently, patient-specific protocols have not been readily employed to significantly reduce contrast media dose during CTPA without compromising image quality (12, 14). Nevertheless, to our knowledge this is the first study to investigate a possible relationship between CMV and lung volumes, weight and BMI and how different CMVs could affect confidence in emboli detection and image quality when employing a patient-specific formula.

The results of this study have demonstrated a significant correlation between CMV and lung organ volumes. When this formula was applied to patients, the CMV increased with increased lung volume which might be important in order to maintain a good visualization of pulmonary vasculature. Also, there was no significant change in CMV with gender and age, however, CMV initially increased with increasing body weight and BMI when patient were unequally grouped into 7 protocol ranges. However when grouped into 3 ranges with same patient number, body weight and BMI did not corelated with CMV which is in contrast with previous findings (26-30). The reduced CMV did not affect pulmonary artery opacification and the sensitivity and specificity of pulmonary emboli detection as those in previously reported papers (31-33).

There still remain controversies surrounding the effect of CMV and increased radiation dose due to the photoelectric effect. Recent studies demonstrated that the addition of contrast media during CT increased double DNA strand breaks which is attributed to increased radiation dose (34, 35). Additionally, future studies published should consider the effect of iodinated contrast material on the organ doses

administered to patients undergoing CT, as it is important in estimating radiation dose (36, 37). In our study, we demonstrated that increased lung volume was correlated with increased CMV as well as radiation dose, but when compared to other studies, our CMV range was from 10 – 76mLs and other studies from 40 – 120mLs (38-42). Finally, a strong correlation between increased lung and contrast volumes, demonstrated no correlation with BMI. Therefore, the radiation dose increase can be attributed to the increased volume in the pulmonary circulation at the time of the CTA and not patient weight.

There were shortcomings in the current study. Firstly, whilst every attempt was made to have uniform inspiration between patient to patient, the exact air volume entering the lungs could not be controlled and thus potentially the increase in blood volume could not be determined. Secondly, we did not measure the effect between weight-based contrast media protocols and the patient-specific contrast media protocols in pulmonary CTA. Finally, the main limitation of this study is the fact that it is a retrospective one. A randomized clinical trial will be needed to confirm our results.

Conclusion

High CMVs present a health hazard that could be avoided if patient specific CMVs are administered. The patient specific CMVs should preserve image quality thus maintaining the diagnostic relevance of their usage. A correlation between CMV and lung volume might be important in order to maintain a good visualization of pulmonary vasculature. This study showed that administering a patient tailored CMV can preserve

image quality. Moreover, increased CMV is significantly correlated to increased patient lung volume when employing a patient-specific contrast formula. The main limitations of this study is the fact that it is a retrospective study. A randomized clinical trial is needed to confirm our results.

References

1. Saade C, Bourne R, El-Merhi F, Somanathan A, Chakraborty D, Brennan P**.** An optimised patient-specific approach to administration of contrast agent for CT pulmonary angiography. Eur Radiol. 2013;23(11):3205-12.
2. Salameh E, Saade C, Oweis GF**.** Experimental Insight into the Hemodynamics and Perfusion of Radiological Contrast in Patent and Non-patent Aortic Dissection Models. Cardiovasc Eng Technol. 2019;10(2):314-28.
3. Saade C, Hamieh N, Deeb IA, Haddad M, Abi-Ghanem AS, Ghieh D, et al. An augmented patient-specific approach to administration of contrast agent for CT renal angiography. Int Braz J Urol. 2019;45.
4. Saade C, Chokr J, Naffaa L, Faraj W, Shamseddine A, Mukherji D, et al. Reduced Contrast Volume and Radiation Dose During Computed Tomography of the Pancreas: Timing-Specific Contrast Media Protocol. Acad Radiol. 2019;26(4):480-8.
5. Zein-El-Dine S, Bou Akl I, Mohamad M, Chmaisse A, Chahwan S, Asmar K, et al. Split-bolus contrast injection protocol enhances the visualization of the thoracic

vasculature and reduced radiation dose during chest CT. Br J Radiol. 2018;91(1092):20180509.

6. Saade C, Mohamad M, Kerek R, Hamieh N, Alsheikh Deeb I, El-Achkar B, et al. Augmented Quadruple-Phase Contrast Media Administration and Triphasic Scan Protocol Increases Image Quality at Reduced Radiation Dose During Computed Tomography Urography. J Comput Assist Tomogr. 2018;42(2):216-21.
7. Saade C, Mayat A, El-Merhi F**.** Exponentially Decelerated Contrast Media Injection Rate Combined With a Novel Patient-Specific Contrast Formula Reduces Contrast Volume Administration and Radiation Dose During Computed Tomography Pulmonary Angiography. J Comput Assist Tomogr. 2016;40(3):370-4.
8. Saade C, El-Merhi F, El-Achkar B, Kerek R, Vogl TJ, Maroun GG, et al. 256 Slice Multi-detector Computed Tomography Thoracic Aorta Computed Tomography Angiography: Improved Luminal Opacification Using a Patient-Specific Contrast Protocol and Caudocranial Scan Acquisition. J Comput Assist Tomogr. 2016;40(6):964-70.
9. Saade C, Al-Hamra S, Al-Mohiy H, El-Merhi F**.** Contrast Media Delivery in the Assessment of Anomalous Left Coronary Artery From the Pulmonary Artery. Radiol Technol. 2016;87(5):490-4.
10. Puybasset L, Cluzel P, Gusman P, Grenier P, Preteux F, Rouby JJ**.** Regional distribution of gas and tissue in acute respiratory distress syndrome. I.

Consequences for lung morphology. CT Scan ARDS Study Group. Intensive Care Med. 2000;26(7):857-69.

11. Gimenez S, Teixeira ML, Myashiro R, Carmona MJ, Auler JO, Jr., Malbouisson LM. [Computed tomography in pulmonary evaluation of children with acyanotic congenital heart defect and pulmonary hyperflow]. Rev Bras Anestesiol. 2009;59(5):545-57.

12. Saade C, Bourne R, El-Merhi F, Somanathan A, Chakraborty D, Brennan P. An optimised patient-specific approach to administration of contrast agent for CT pulmonary angiography. European radiology. 2013;23(11):3205-12.

13. Saade C, Bourne R, Wilkinson M, Brennan P. Contrast medium administration and parameters affecting bolus geometry in multidetector computed tomography angiography: an overview. Journal of Medical Imaging and Radiation Sciences. 2011;42(3):113-7.

14. Saade C, Mayat A, El-Merhi F. Exponentially decelerated contrast media injection rate combined with a novel patient-specific contrast formula reduces contrast volume administration and radiation dose during computed tomography pulmonary angiography. Journal of computer assisted tomography. 2016;40(3):370-4.

15. Hittmair K, Fleischmann D. Accuracy of predicting and controlling time-dependent aortic enhancement from a test bolus injection. Journal of computer assisted tomography. 2001;25(2):287-94.

16. You SY, Yoon DY, Choi CS, Chang SK, Yun EJ, Seo YL, et al. Effects of right- versus left-arm injections of contrast material on computed tomography of the head and neck. Journal of computer assisted tomography. 2007;31(5):677-81.

17. Saade C, Bourne R, Wilkinson M, Brennan P**.** Cardiovascular CTA applications: patient-specific contrast formulae. Proc. of SPIE Vol, 2013. 86731R-1.

18. Huda W, Ogden KM, Khorasani MR**.** Converting dose-length product to effective dose at CT. Radiology. 2008;248(3):995-1003.

19. Brennan PC, McEntee M, Evanoff M, Phillips P, O'Connor WT, Manning DJ**.** Ambient lighting: effect of illumination on soft-copy viewing of radiographs of the wrist. AJR. American journal of roentgenology. 2007;188(2):W177-80.

20. Charbel Saade RB, Mark Wilkinson, Michael Evanoffb,, Patrick Brennan**.** A reduced contrast volume acquisition regimen based on cardiovascular dynamics improves visualisation of head and neck vasculature with carotid MDCT angiography. European journal of radiology. 2012.

21. Bath M, Mansson LG**.** Visual grading characteristics (VGC) analysis: a non-parametric rank-invariant statistical method for image quality evaluation. The British journal of radiology. 2007;80(951):169-76.

22. McDermott S, Otrakji A, Flores EJ, Kalra MK, Shepard J-AO, Digumarthy SR**.** Should Dual-Energy Computed Tomography Pulmonary Angiography Replace Single-Energy Computed Tomography Pulmonary Angiography in Pregnant and Postpartum Patients? Journal of computer assisted tomography. 2018;42(1):25-32.

23. Li X, Chen GZ, Zhao YE, Schoepf UJ, Albrecht MH, Bickford MW, et al. Radiation optimized dual-source dual-energy computed tomography pulmonary angiography: intra-individual and inter-individual comparison. Academic Radiology. 2017;24(1):13-21.

24. Aschoff AJ, Catalano C, Kirchin MA, Krix M, Albrecht T**.** Low radiation dose in computed tomography: the role of iodine. The British Journal of Radiology. 2017;90(0):20170079.

25. Bae KT**.** Intravenous contrast medium administration and scan timing at CT: considerations and approaches. Radiology. 2010;256(1):32-61.

26. Sahebjami H**.** Dyspnea in obese healthy men. Chest. 1998;114(5):1373-7.

27. Ray CS, Sue DY, Bray G, Hansen JE, Wasserman K**.** Effects of obesity on respiratory function. Am Rev Respir Dis. 1983;128(3):501-6.

28. Jenkins SC, Moxham J**.** The effects of mild obesity on lung function. Respir Med. 1991;85(4):309-11.

29. Rubinstein I, Zamel N, DuBarry L, Hoffstein V**.** Airflow limitation in morbidly obese, nonsmoking men. Ann Intern Med. 1990;112(11):828-32.

30. Bedell GN, Wilson WR, Seebohm PM**.** Pulmonary function in obese persons. J Clin Invest. 1958;37(7):1049-60.

31. Bass AR, Fields KG, Goto R, Turissini G, Dey S, Russell LA**.** Clinical Decision Rules for Pulmonary Embolism in Hospitalized Patients: A Systematic Literature Review and Meta-analysis. Thrombosis and haemostasis. 2017;117(11):2176-85.

32. Milà M, Bechini J, Vázquez A, Vallejos V, Tenesa M, Espinal A, et al. Acute pulmonary embolism detection with ventilation/perfusion SPECT combined with full dose CT: What is the best option? Revista Española de Medicina Nuclear e Imagen Molecular. 2017;36(3):139-45.

33. Takx RA, Henzler T, Schoepf UJ, Germann T, Schoenberg SO, Shirinova A, et al. Predictive value of perfusion defects on dual energy CTA in the absence of thromboembolic clots. Journal of Cardiovascular Computed Tomography. 2017;11(3):183-7.

34. Piechowiak EI, Peter J-FW, Kleb B, Klose KJ, Heverhagen JT. Intravenous iodinated contrast agents amplify DNA radiation damage at CT. Radiology. 2015;275(3):692-7.

35. Kuefner M, Brand M, Engert C, Schwab S, Uder M. Radiation induced DNA double-strand breaks in radiology. RöFo-Fortschritte auf dem Gebiet der Röntgenstrahlen und der bildgebenden Verfahren, 2015. © Georg Thieme Verlag KG: 872-8.

36. Sahbaee P, Segars WP, Marin D, Nelson RC, Samei E. The effect of contrast material on radiation dose at CT: part I. Incorporation of contrast material dynamics in anthropomorphic phantoms. Radiology. 2017;283(3):739-48.

37. Sahbaee P, Abadi E, Segars WP, Marin D, Nelson RC, Samei E. The Effect of Contrast Material on Radiation Dose at CT: Part II—A Systematic Evaluation across 58 Patient Models. Radiology. 2017:152852.

38. Laqmani A, Kurfurst M, Butscheidt S, Sehner S, Schmidt-Holtz J, Behzadi C, et al. CT Pulmonary Angiography at Reduced Radiation Exposure and Contrast Material Volume Using Iterative Model Reconstruction and iDose4 Technique in Comparison to FBP. PLoS One. 2016;11(9):e0162429.

39. Kerl JM, Lehnert T, Schell B, Bodelle B, Beeres M, Jacobi V, et al. Intravenous contrast material administration at high-pitch dual-source CT pulmonary angiography: test bolus versus bolus-tracking technique. Eur J Radiol. 2012;81(10):2887-91.

40. Damm R, Mohnike K, Gazis A, Rogits B, Seidensticker M, Ricke J, et al. Improvement of Contrast Media Enhancement in CTA Evaluating Pulmonary Embolism by Utilizing 'Delayed'Bolus Tracking in the Descending Aorta. Polish journal of radiology. 2016;81:422.

41. Zapala MA, Zurakowski D, Lee EY**.** Comparison of mechanical versus hand administration of IV contrast agents for pediatric pulmonary CT angiography. American Journal of Roentgenology. 2017;208(3):632-6.

42. Mourits M, Nijhof W, van Leuken M, Jager G, Rutten M**.** Reducing contrast medium volume and tube voltage in CT angiography of the pulmonary artery. Clinical radiology. 2016;71(6):615. e7-. e13.